COO-1051-45

MASTER

THEORETICAL STUDY OF ELASTIC AND INELASTIC PION-^{12}C SCATTERING AT INTERMEDIATE ENERGIES†

H. K. Lee‡

California State College, Dominguez Hills, California

and

H. McManus

Michigan State University, East Lansing, Michigan

Submitted to Nuclear Physics B
December, 1970

ABSTRACT

Elastic and inelastic cross sections are computed using the distorted wave impulse approximation. The WKB method and a modified distorted wave code are compared. As input, we use pion-nucleon phase shifts, nucleon density from electron scattering, and microscopic inelastic form factors. It is found that the interaction given by the impulse approximation gives a fair fit to the elastic data and that the WKB approximation compares remarkably well with the distorted wave calculation at all but the lowest energies. The microscopic form

---

†Work supported in part by U. S. Atomic Energy Commission.

‡Supported by a research grant from California State College, Dominguez Hills, California.

DISCLAIMER

factors of the 2^+ level at 4.4 MeV and 3^- level at 9.6 MeV give a good account of the inelastic scattering. Discrepancies in the elastic scattering are similar to those observed in 1 GeV proton scattering from Carbon.

1. INTRODUCTION

Various authors have investigated pion-nucleus scattering for the purpose of studying nuclear structure and the pion-nucleon interaction inside the nucleus. (For a review of the field, see ref. [1].) Kisslinger [2] introduced a gradient term in the optical potential to account for the rise of the cross section at large angles in pion-carbon scattering at 62 MeV. A similar gradient term was found to be essential in reproducing the data at 80 MeV [3]. Auerbach, Fleming and Sternheim applied the same type of potential to obtain reasonably good fits to data in the 20-150 MeV range [4]. However, Block and Koetke found that a simple impulse approximation worked well in explaining pion-helium data at 24 MeV, when the extra absorption of pions by the helium nucleus was included [5]. Recently, Bion et al. [6] measured the elastic and inelastic cross sections of 120-280 MeV pions scattered from ^{12}C. Krell and Barmo and also Sternheim and Auerbach [7] used the Kisslinger potential to fit the above pion-carbon elastic data. Schmit and also K. Bjørnenak et al., have applied the Glauber approximation to analyze the same elastic data [8].

The purpose of the present paper is to study the recent elastic and inelastic data [6] using the impulse approximation. The elastic cross sections are calculated by two independent methods, the WKB approximation and a modified distorted wave code by Tamura. It is interesting to compare the WKB approximation, which is a high energy and small angle approximation, with the "exact" distorted wave code at these intermediate energies. The inelastic cross section for 2^+ and 3^- states are computed by the WKB-Glauber formalism. Microscopic inelastic form factors are used. There are no free parameters in the calculations.

2. OUTLINE OF CALCULATIONS

The optical potential is computed to lowest order, ignoring the antisymmetrization of the target nucleons, and off-shell effects for pion-nucleon scattering [9].

$$U(r) = \frac{A}{(2\pi)^3} \int \langle \underset{\sim}{k}' | t | \underset{\sim}{k} \rangle F(q) e^{i \underset{\sim}{q} \cdot \underset{\sim}{r}} d^3 q \tag{1}$$

where $\underset{\sim}{k}$ and $\underset{\sim}{k}'$ are the initial and final pion momenta in the pion-nucleus CM system and F(q) is the Fourier transform of the normalized nucleon density, i.e.,

$$F(q) = \int \rho(r) e^{-i \underset{\sim}{q} \cdot \underset{\sim}{r}} d^3 r \tag{2}$$

$$\rho(r) = \rho_0(1+{}^{\alpha r^2}/{}_{a^2})\exp({}^{-r^2}/{}_{a_c^2}) \qquad (3)$$

$<\underset{\sim}{k}'|t|\underset{\sim}{k}>$ is the pion-nucleon transition matrix in the pion-nucleus center of mass system. A is the number of nucleons in the target. We relate $<\underset{\sim}{k}'|t|\underset{\sim}{k}>$ to the t matrix in the pion-nucleon CM system [9] by

$$\sqrt{E'E_1'}\ <\underset{\sim}{k}'|t|\underset{\sim}{k}>\ \sqrt{EE_1} = \sqrt{E_0'E_{10}'}\ <\underset{\sim}{k}_0'|t|\underset{\sim}{k}_0>\ \sqrt{E_0E_{10}} \qquad (4)$$

where E, E_1, E', E_1' are the energies of the pion and nucleon before and after the collision. The subscript 0 indicates the corresponding quantitites in the pion-nucleon CM system. The t matrices are related to the scattering amplitudes in the pion-nucleon CM system via

$$f(k_0,q) = -\frac{1}{2\pi}\cdot\frac{E_0E_{10}}{E_0+E_{10}}<\underset{\sim}{k}_0'|t|\underset{\sim}{k}_0> \qquad (5)$$

$$\frac{d\sigma}{d\Omega} = |f|^2 \qquad \underset{\sim}{q} = \underset{\sim}{k}_0-\underset{\sim}{k}_0' \qquad (6)$$

Now, we can write f in terms of the nucleon spin operator $\underset{\sim}{\sigma}$, and the pion and nucleon isospin operators $\underset{\sim}{i}$ and $\underset{\sim}{\tau}$ [1].

$$f = f_0 + f_1\ \underset{\sim}{i}\cdot\underset{\sim}{\tau} + \underset{\sim}{\sigma}\cdot\underset{\sim}{n}[f_2 + f_3\ \underset{\sim}{i}\cdot\underset{\sim}{\tau}] \qquad (7)$$

$\underset{\sim}{n}$ is the unit vector perpendicular to the scattering plane. The coefficients f_i are found from the pion-nucleon phase shifts $\delta^{\ell}_{2I,2j}$ where ℓ,I,j are the quantum numbers of the orbital angular momentum, isospin, and the total angular momentum of the pion-nucleon system. Define

$$\alpha^{\ell}_{2I,2j} = \sin(\delta^{\ell}_{2I,2j})\exp(i\delta^{\ell}_{2I,2j}) \tag{8}$$

Then,

$$f_0 = {}^{1}/_{3k_0} \sum_{\ell=0} [\ell(\alpha^{\ell}_{1,2\ell-1} + 2\alpha^{\ell}_{3,2\ell-1}) + (\ell+1)(\alpha^{\ell}_{1,2\ell+1} + 2\alpha^{\ell}_{3,2\ell+1})] \times P_{\ell}(\cos\theta) \tag{9}$$

$$f_1 = {}^{1}/_{3k_0} \sum_{\ell=0} [\ell(-\alpha^{\ell}_{1,2\ell-1} + \alpha^{\ell}_{3,2\ell-1}) + (\ell+1)(-\alpha^{\ell}_{1,2\ell+1} + \alpha^{\ell}_{3,2\ell+1})] \times P_{\ell}(\cos\theta) \tag{10}$$

$$f_2 = i\ \sin\theta/_{3k_0} \sum_{\ell=0} [-\alpha^{\ell}_{1,2\ell-1} - 2\alpha^{\ell}_{3,2\ell-1} + \alpha^{\ell}_{1,2\ell+1} + 2\alpha^{\ell}_{3,2\ell+1}] P'_{\ell} \tag{11}$$

$$f_3 = i\ \sin\theta/_{3k_0} \sum_{\ell=0} [\alpha^{\ell}_{1,2\ell-1} - \alpha^{\ell}_{3,2\ell-1} - \alpha^{\ell}_{1,2\ell+1} + \alpha^{\ell}_{3,2\ell+1}] P'_{\ell} \tag{12}$$

The functions P_{ℓ} are the Legendre polynomials and

$$P'_{\ell} = \frac{dP_{\ell}(t)}{dt} \qquad t = \cos\theta$$

For the optical potential, we take the average of f over the spin and isospin of the ^{12}C ground state, which has T = J = 0. Since

$$\langle T=0 | \sum_{j=1}^{A} \tau_j | T=0 \rangle = \langle J=0 | \sum_{j=1}^{A} \sigma_j | J=0 \rangle = 0 \tag{13}$$

in the present approximation, in which we ignore the anti-symmetrization of the target nucleons, only f_0 contributes to the optical potential. We keep the terms in eqs. (9) - (12)

up to and including $\ell = 3$. The phase-shifts are taken from Roper, Wright and Field [10]. The parameters for the proton point density (3) are deduced from electron scattering [11],

$$\alpha = 4/3, \qquad a = 1.66 \text{ fm}, \qquad a_c = 1.66 \text{ fm}$$

These constants are also used for the neutron density.

The elastic scattering amplitude is, in the WKB approximation [12],

$$S = \exp(i\chi_s)\{f_{pt}(q) - ik\int_0^\infty J_0(qb)[\exp(i\chi(b)+i\chi_\rho(b)) - \exp(i\chi_{pt}(b))]bdb\} \tag{14}$$

where $f_{pt}(q)$ is the usual Rutherford scattering due to a point charge Ze and

$$\chi(b) = -\frac{E}{k}\int_{-0}^{\infty} U(\underset{\sim}{b},z)dz \tag{15}$$

$\underset{\sim}{b}$ is the impact parameter. χ_{pt} and χ_ρ are the same as χ with U replaced by the Coulomb potentials due respectively to a point charge and a charge distribution of the form of eq. (3) with a_c= 1.71 fm, corresponding to a charge radius of 2.5 fm [11]. χ_s is a real constant factor which depends on the cut-off radius of the Coulomb potential of a screened point charge.

The elastic cross sections were also calculated with Tamura's distorted wave code using the same optical potential, but without Coulomb. This code was originally written for proton-nucleus scattering at lower energies but was suitably modified for pion-nucleus scattering at relativistic energies.

The inelastic scattering amplitude for a transition to the state $|L, S, J, \mu\rangle$ is in the WKB-Glauber formalism [13, 14],

$$S(L, S, J,\mu) = \frac{ik}{2\pi} \int \exp(i\underset{\sim}{q}\cdot\underset{\sim}{b}+i\chi(b)) \times \langle L,S,J,\mu| \sum_{j=1}^{A} \Gamma(\underset{\sim}{b}-\underset{\sim}{s}_j)\,|0\rangle d^2b \qquad (16)$$

where μ is the z component of the total angular momentum J, and

$$\Gamma(\underset{\sim}{b}-\underset{\sim}{s}_j) = \frac{1}{2\pi i k_0} \int \exp(-i\underset{\sim}{\delta}\cdot(\underset{\sim}{b}-\underset{\sim}{s}_j)) f(k_0,\delta) d^2\delta$$

Since the final states we are interested in have isospin T = 0, only f_0 and f_2 contribute due to eq. (13). For the final state S = 0, L = J, and T=0, we have

$$S(L,0,J,\mu) = \frac{ik}{2\pi} \int \exp(i\underset{\sim}{q}\cdot\underset{\sim}{b}+i\chi(\underset{\sim}{b}) d^2b [\frac{1}{2\pi i k_0} \int \exp(-i\underset{\sim}{\delta}\cdot\underset{\sim}{b}) f_0(k_0,\underset{\sim}{\delta}) d^2\delta \int \exp(i\underset{\sim}{\delta}\cdot\underset{\sim}{s}') F^{LOJ}(r') Y^{*}_{L,\mu}(\theta',\phi') d^3r'] \qquad (17)$$

When the final state has S = 1, L = J, and T=0,

$$S(L,1,J,\mu) = \frac{ik}{2\pi} \int \exp(i\underset{\sim}{q}\cdot\underset{\sim}{b}+i\chi(\underset{\sim}{b}))d^2b[\frac{1}{2\pi i k_0} \int$$

$$\exp(-i\underset{\sim}{\delta}\cdot\underset{\sim}{b})f_2(k_0,\underset{\sim}{\delta})d^2\delta \sum_{M_1,M_2} \langle L,1,M_1,M_2|J,\mu\rangle i(\delta_{M_2,1}$$

$$+\delta_{M_2,-1}) \int \exp(i\underset{\sim}{\delta}\cdot\underset{\sim}{s}')F^{L1J}(r')Y^*_{L,\mu}(\theta',\phi')d^3r' \tag{18}$$

where $\underset{\sim}{r}' = (\underset{\sim}{s}', z') = (r',\theta',\phi')$,

and M_1 and M_2 are the z components of L and S. The inelastic form factors F^{LSJ} are defined in terms of the reduced transition matrix and have been computed from the Gillet particle-hole model [13, 15]. For the 2^+ state at 4.4 MeV,

$$F^{202} = 0.225(\alpha_1)^{5/2}(5.52r^2-0.183\alpha_1 r^4) \exp(-\alpha_1 r^2)$$

$$F^{212} = 0.225(\alpha_1)^{5/2}(-3.54r^2+0.665\alpha_1 r^4) \exp(-\alpha_1 r^2)$$

and for the 3^- state at 9.6 MeV,

$$F^{303} = -0.545\alpha_1^3 r^3 \exp(-\alpha_1 r^2)$$

$$F^{313} = 0.178\alpha_1^3 r^3 \exp(-\alpha_1 r^2)$$

with

$$\alpha_1 = 0.37 \text{ fm}^{-2}.$$

3. DISCUSSION

The optical potentials U have been computed using eq. (1) and are shown in figure 1. The low energy real potentials U_R are comparable in magnitude with the incident energy, $U_R/E \tilde{=} 1$, violating a necessary condition for the WKB approximation. However, since the strong imaginary potentials U_I will depress the scattering from these regions, we can still expect the WKB method to work at least for some of the low incident energies. The real parts (U_R) are attractive up to and including 180 MeV and repulsive thereafter. The optical potentials show considerable deviations in shape from the standard potentials encountered in proton-nucleus scattering. To understand the unusual shapes, we write, assuming only s and p wave contributions to f_0,

$$f_0 = f_{01} + f_{02}q^2$$

Then, from (1), (4), and (5),

$$\begin{aligned} U &= -C\int F(q)\,(f_{01}(k_0)+f_{02}(k_0)q^2)\exp(i\underset{\sim}{q}\cdot\underset{\sim}{r})\,d^3q \\ &= -Cf_{01}\rho(r)+Cf_{02}\nabla^2\rho(r) = U_0+W \end{aligned} \qquad (19)$$

where

$$U_0 = -Cf_{01}\rho(r) \qquad\qquad W = Cf_{02}\nabla^2\rho(r)$$

$$C = \frac{A}{(2\pi)^2}\;\frac{k}{E}\,\frac{1}{k_0}$$

As the pion-nucleon interaction varies rapidly with energy in the energy range considered, it must give rise to a non-local optical potential which is approximated in the present work by a sum of local potentials U_0 and W both of which have energy dependent parameters. The first of these, U_0, the quasi-local part, comes from a zero range interaction giving rise to an optical potential U_{OR} and U_{OI} (the real and imaginary parts of U_0) which have the same shape as the density distribution, i.e. a modified gaussian. The second, W, has an extra non-locality indicated by its proportionality to $\nabla^2\rho$ which makes it very sensitive to the density distribution assumed. W has significant contributions where the change of the slope of $\rho(r)$ is great. That is,

$$W = C\ f_{02}\rho_0 g(r)\ \exp(-\beta r^2)$$

$$g(r) = 6(\rho_1-\beta)-(14\beta\rho_1-4\beta^2)r^2+4\beta^2\rho_1 r^4$$

where

$$\beta = 1/a^2 \qquad \rho_1 = 4\beta/3 \qquad a = 1.66\ \text{fm}$$

g(r) has a positive maximum at r = 0, a minimum (negative) at r = 1.5 fm, and zeroes at r = 0.63 fm and 2.7 fm. The plots of U_R and U_I, the real and imaginary parts of the total optical potential U, when compared with U_{OR} U_{OI} reflect these features. The contribution of W is most signigicant at lower energies, which explains the reason why the usual optical potential fails at low energies [13]. We have calculated the root mean square radii of U_R and U_I by

$$\langle r^2 \rangle^{1/2} = \left(\int U r^2 d^3 r \Big/ \int U d^3 r \right)^{1/2}$$

We note that the rms radii of U, as tabulated in Table 1, decrease with energy except near the (3,3) resonance and appear to converge to those of U_0. The rms radii of U_{OR} and U_{OI} are 2.45 fm at all energies. The effect of the extra non-locality contained in W is to add a grey penumbra to the black sphere which is the main feature of the optical potential. The penumbra shrinks as the energy increases and the total optical potential is approaching the quasi local potential U_0 at 280 MeV.

The elastic cross sections were calculated four times at each energy and are shown in figure 2, compared with the experimental results of Binon <u>et al</u>. The solid line is the cross section obtained by using a distorted wave calculation with the full optical potential but without Coulomb interaction. The dashed curve is a WKB calculation using the full optical potential with Coulomb; the dotted line is a WKB calculation using the full optical potential without Coulomb; and the dashed line with crosses is the WKB calculation with the quasi local potential U_0 only.

The inelastic cross sections to the 2^+, (Q=4.4 MeV) and 3^- (Q=9.6 MeV) states were calculated using the WKB-Glauber method with the full optical potential. They are plotted in comparison with the experimental results of Binon <u>et al</u>. in figure 3.

If we look at the lowest energy considered, 120 MeV, we find that the modified Tamura code gives a reasonably good fit to the elastic scattering while the success of the WKB at this energy is marginal. We see the importance of W as the prediction of U_0 alone fails badly at larger angles. The Coulomb interference is constructive at both forward angles and at the minimum as both pion-nucleon and Coulomb forces are attractive. The peak in the 2^+ cross section occurs at $q = 0.9$ fm^{-1}. This value is in good agreement with the 156 MeV proton inelastic scattering [13] and smaller than $q = 1.2$ fm^{-1} for the peaks in 1 GeV proton inelastic scattering [16] and in electron scattering [17]. This discrepancy reflects the difference between the ranges of the pion-nucleon interaction at 120 MeV and the nucleon-nucleon interaction at 150 MeV which has $r_d^2 = 4$ fm^2 and the ranges of the nucleon-nucleon interaction at 1 GeV and the proton electromagnetic form factor, both of which have $r_d^2 =$ 0.6 fm^2, where r_d^2 is the mean square radius of the hadron-hadron interaction or electromagnetic form factor. The dip in the cross section at 70° is due to the largely p-wave character of the pion-nucleon amplitude. The pion-nucleon amplitude has a minimum at $\theta_0 = 90°$ in the pion-nucleon center of mass which corresponds to an angle $\theta_{cm} = 72°$ in the pion-carbon CM system. The 3^- inelastic data are not available at this energy.

At 150 MeV the predicted cross sections are in reasonably good accord with the elastic data except near the first minimum and the second peak. It is interesting to note that similar discrepancies appear in 1 GeV proton carbon scattering [16] and in the pion scattering analysis using the Kisslinger potential by Krell and Barmo [7]. The agreement between the WKB and modified distorted wave code is good. The strong diffraction features are due to the large imaginary potential compared to the real part. The potential U_0 gives good agreement up to 60° including the first minimum but too large cross sections at larger angles. This is consistent with the fact that the rms radii of U_0 are smaller than those of U. The agreement between theory and experiment is good for both 2^+ and 3^- states. The 3^- maximum occurs at $q = 1.1 fm^{-1}$, which, like the 2^+ state, is in good accord with the 156 MeV proton scattering but is less than the $q=1.4fm^{-1}$, given by 1 GeV proton and electron scattering, rendering evidence again, as for the scattering of 120 MeV pions exciting the 2^+ state, of the different ranges of the two body forces for different projectiles at different energies. The inelastic cross-sections thus do show some sensitivity to the range of the various forces. The spin-flip contribution, F^{LiJ}, to the inelastic scattering is negligible except for a 20% effect near the minimum where the significance of the changes in the small numbers is questionable.

At 180 MeV the optical potential is largely imaginary, which explains the sharp diffraction structures in both the elastic and inelastic data. The agreement between the calculations (both Tamura and WKB) and the elastic data is good except, again, at the minimum. The Coulomb interference is almost zero in the forward direction due to the very small real optical potential. Again, the potential U_0 is successful in giving the correct minimum position. Also, there is a reasonably good agreement between predictions and data for inelastic scattering.

A new feature at 200 MeV is that the real part of the optical potential is repulsive, which is evidenced by the destructive interference in the forward direction and at the minima in figure 2. The minima are beginning to "fill-up" due to the sizeable U_R. The potential U_0 does remarkably well up to the first peak and is able to produce the second minimum, although at too large an angle. Discussions regarding the inelastic scattering are similar to the previous ones except for the fact that the height of the predicted cross sections is slightly too low.

At the higher energies (230, 260 and 280 MeV) both the shape and the rms radii of U are approaching U_0 although significant differences persist even at 280 MeV. The optical potential U predicts cross sections that are too small at large angles, while U_0 gives a good fit at 280 MeV. It would be interesting to see whether U_0 would continue to give a good fit beyond 300 MeV. The trend suggests that the usual optical potential of modified Gaussian or Wood-Saxon shape should work well at energies beyond 300 MeV. To attempt to compare U and U_0 in further detail would take us beyond the limit of the assumptions of eq. (1). The contributions of the d and f phase-shifts are small at 230 MeV but are sizeable at 280 MeV. That is, we find that omission of these phase-shifts would increase the cross section by ~30% near the first minimum and depress it by ~15% at larger angles. The 2^+ and 3^- form factors continue to give reasonable agreement with the data.

4. CONCLUSIONS

First, we find that optical potentials which are obtained with the impulse approximation and contain no free parameters give fair fits to the existing data in the range 120-280 MeV. The term W which is proportional to the second derivative of $\rho(r)$ is essential at the lower energies. The quality of the fits are as good as those obtained by Krell and Barmo [7] who searched for the best parameters of the Kisslinger potential. It is evident that the simple approximation using $\nabla^2\rho$ works as well as the corresponding terms in the Kisslinger potential.

Secondly, the WKB method works remarkably well for elastic scattering in comparison with a distorted wave code for 150 MeV incident energy and above. The reason for such success at these intermediate energies is believed to be the strong imaginary part of the optical potential. Nevertheless, there are distinct differences between the WKB and the distorted wave calculation in the depths of the minima and heights of secondary maxima at large momentum transfers, a fact which has to be kept in mind if the heights at minimum are used as criteria for the existence of higher order effects such as correlations in an approximate calculation.

Thirdly, we see that for elastic scattering, except at the lowest energy, there is a persistant discrepancy between the calculated and experimental results in that theory gives the first minimum and the secondary maximum consistently at too low a momentum transfer, as if the nucleus was somewhat smaller than that given by theory. The same discrepancy was found by Krell and Barmo [7]. Taken at its face value and given the fact that the zero range interaction U_0 gives a good fit at high energies, this would suggest that the present local approximation exaggerates the non-locality of U and that a smooth short range interaction would be more realistic. A Glauber type approximation by K. Bjørnenak et al. [8] which neglects some of the momentum dependence of the two body amplitude but makes up for it by averaging over the nuclear fermi motion, goes in the opposite direction, predicting the minima at too large a momentum transfer. This calculation kept p-waves only in the pion-nucleon interaction, and used antisymmetrized wave-functions which gave small contributions from the spin-flip part of the amplitudes, and so is not directly comparable to the present calculation. A recent calculation by Sternheim and Auerbach [7] used the Kisslinger form of the optical potential obtained from the pion-nucleon s and p wave phase shifts, but averaged over the Fermi motion of the nucleons. They did not find any discrepancies in the position of the first minimum, but they used for the nucleon point density a distribution of the form (3) but with the parameters a = 1.5 fm and a_c = 1.5 fm taken from an earlier analysis of electron scattering, instead of the 1.66 fm used in the present calculation. Their parameters correspond to a nucleus about 10% smaller than the one assumed in the present work and would move the first minima in figure 2 outwards by a corresponding amount. Thus most of the discrepancy between the two calculations comes from the difference in matter radius. It should be remembered that a very similar discrepancy to the one found here occurs between theory and experiment in the scattering of 1 GeV protons from ^{12}C, whereas no such discrepancy occurs from a similar comparison involving O^{16} as target, as has been noted by several authors [16, 18], all of whom used the same parameters for ^{12}C as used here. The discrepancy has been taken to mean that the ground state of ^{12}C is deformed, or that as the 2^+(4.4 MeV) state of ^{12}C is strongly excited at all energies, a coupled channel calculation may be necessary for hadron scattering, even if the corresponding dispersive corrections for electron scattering are very small. In any case, it needs to be determined whether there is a nucleon distribution in ^{12}C which is compatible with both electron scattering and hadron scattering before significance can be attached to more refined calculations. It would be very convenient to have data in the same energy region for elastic pion scattering from ^{16}O, which shows no anomalies in 1 GeV proton scattering, so that the nuclear structure problem is removed from the picture, and a better test of the two-body interaction could be obtained. A calculation of second order contributions to the optical potential, including corrections to the hadron-hadron scattering amplitudes and the effects of nuclear correlations, along the lines set out by Feshbach and Hufner [19] would be of interest, however, in establishing the convergence of the method for such strong interactions. These second order corrections have been shown [20] to be relatively small except at large momentum transfer, in the case of the scattering of 1 GeV protons from ^{16}O, but are expected to be considerably larger in the present case.

Finally, the 2^+ and 3^- inelastic form factors based on the Gillet particle-hole picture give reasonably good fits for the pion inelastic scattering as they did for 156 MeV [13] and 1 GeV proton scattering [16] and for electron scattering [17] within the errors of the experimental data. The momentum transfer at the maxima in the cross section for these levels gives some indication of the range for two body force involved, but inelastic scattering is not as sensitive to the details as elastic scattering.

The authors wish to thank F. Petrovich for assistance with the distorted wave code, and both the staffs at the Σ7 computer of the MSU cyclotron and at the computer center of California State College, Domingüez Hills, for their cooperation.

REFERENCES

[1] D. S. Koltun, Interaction of Pions with Nuclei, Advances in Nuclear Physics, Vol. 3 (Academic Press, New York, 1970).

[2] L. S. Kisslinger, Phys. Rev. 98(1955)761.

[3] W. F. Baker, H. Byfield, and J. Rainwater, Phys. Rev. 122(1958)1773.

[4] E. H. Auerbach, D. M. Fleming, and M. M. Sternheim, Phys. Rev. 162(1967)1683.

[5] M. M. Block and D. Koetke, Nucl. Phys. B5(1968)451.

[6] F. Binon, P. Duteil, J. P. Garron, J. Gorres, L. Hugon, J. P. Peigneux, C. Schmit, M. Spighel, and J. P. Stroot, Nucl. Phys. B17(1970)168.

[7] M. Krell and S. Barmo, Nucl. Phys. B20(1970)461.
M. Sternheim and E. Auerbach, Phys. Rev. Lett 25(1970) 1500.

[8] C. Schmit, Lett. Al Nuovo Cimento, 4, no. 10 (1970)454;
K. Bjørnenak, J. Finjord, P. Osland, and A. Reitan, Nucl. Phys. B22(1970)179.

[9] A. K. Kerman, H. McManus and R. M. Thaler, Ann. of Phys. 8(1959)564.

[10] L. D. Roper, R. M. Wright and B. T. Feld, Phys. Rev. 138B(1965)190.

[11] H. F. Ehrenber, R. Hofstadter, U. Meyer-Berkhout, D. G. Ravenhall, and S. E. Sobottka, Phys. Rev. 113(1959)666.

[12] R. J. Glauber, Theory of high energy hadron-nucleus collisions, High Energy Physics and Nuclear Structure, S. Devons ed., (Plenum Press, New York, 1970).

[13] H. K. Lee and H. McManus, Phys. Rev. 161, No. 4 (1967) 1087.

[14] T. Erickson, Nucl. Phys. 54(1964)231.

[15] V. Gillet and N. Vinh-Mau, Nucl. Phys. 54(1964)321.

[16] H. K. Lee and H. McManus, Phys. Rev. Lett. 20, No. 7 (1968)337. R. H. Bassel and C. Wilkin, Phys. Rev. 174 (1968)1179. W. Czyz and L. C. Maximon, Ann. of Phys. 52(1969)59. L. Lesniak and H. Wolek, Nucl. Phys. A125 (1969)665.

[17] V. Gillet and M. A. Melkanoff, Phys. Rev. 133, 5B (1964) B1190.

[18] H. Palevsky, J. L. Friedes, R. J. Sutter, G. J. Igo, W. D. Simpson, G. C. Phillips, D. M. Corly, N. S. Wall, R. L. Stearns, and B. Gottschalk, Phys. Rev. Lett. 18 (1967)1200.

[19] H. Feshbach and J. Hufner, Ann. of Phys. 56(1970)268.

[20] H. Feshbach, A. Gal and J. Hufner, Ann. of Phys. (to be published).

Table 1. The root mean square radii of the optical potentials. The rms value of U_R at 180 MeV is not calculated. The rms radii of U_0, are 2.45 fm for both real and imaginary parts at all energies.

TABLE 1

	120 MeV	150	180	200	230	260	280
U_R	3.2 fm	3.05		2.64	2.66	2.6	2.56
U_I	3.1 fm	2.96	2.88	2.84	2.87	2.72	2.7

FIGURE CAPTIONS

Fig. 1. Optical Potentials for pions of different incident energies. U_R and U_I are the real and imaginary parts of the full optical potential; U_{OR}, U_{OI} the quasi-local parts only as defined in the text. The notation $\pm U_R$ $\pm U_{OR}$ indicates that the real parts of the optical potentials change from attractive to repulsive after 180 MeV.

Fig. 2. Comparison of theory with experiment for pion-carbon elastic scattering. The experimental points are those of Binon et al. The solid line is the distorted wave calculation, without Coulomb, the dashed line the WKB approximation with Coulomb, the dotted line the WKB calculation without Coulomb, and the crosses indicate a WKB calculation using the quasi-local potentials U_0 only as defined in the text.

Fig. 3. Comparison of theory with experiment for pion-carbon inelastic leaving the target in the 2^+ state ($Q = 4.4$ MeV) and the 3^- state ($Q = 9.6$ MeV).

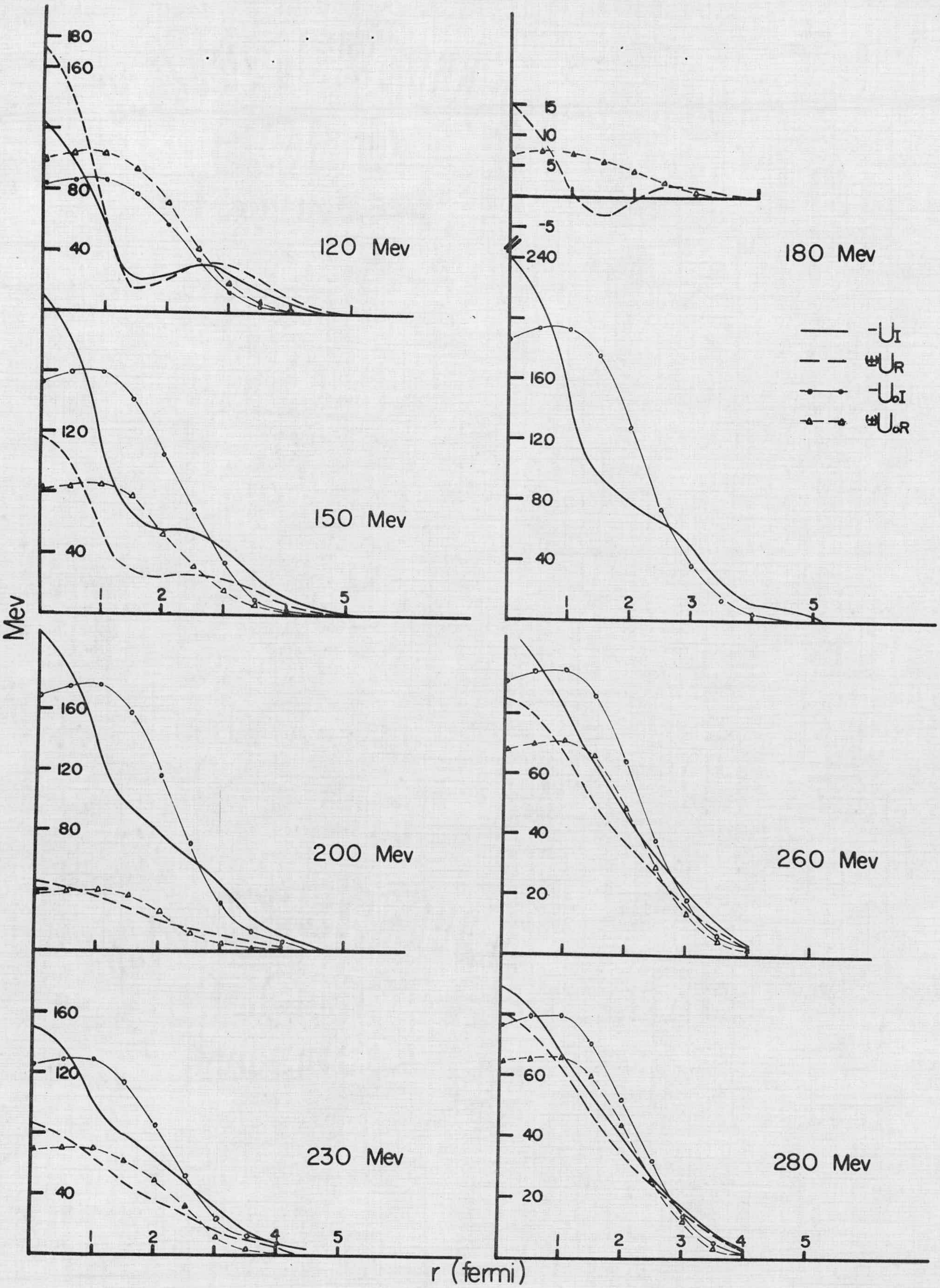

120 Mev
150 Mev
200 Mev
230 Mev
180 Mev
260 Mev
280 Mev
Mev
r (fermi)
$-U_I$
$\mp U_R$
$-U_{oI}$
$\mp U_{oR}$

Figure 1

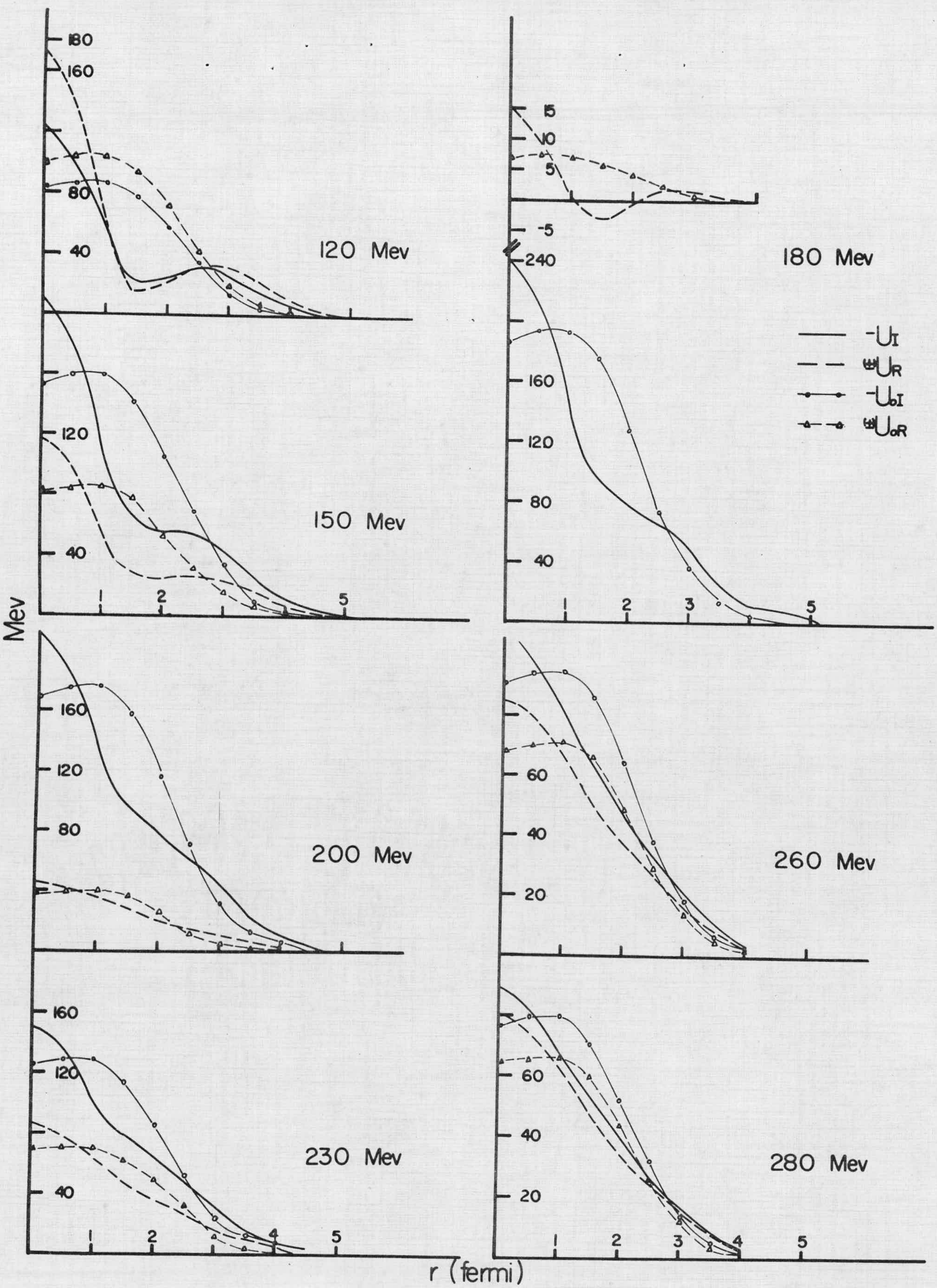

Mev
r (fermi)
120 Mev
150 Mev
200 Mev
230 Mev
180 Mev
260 Mev
280 Mev
-U_I
-U_R
-U_oI
-U_oR

Figure 1

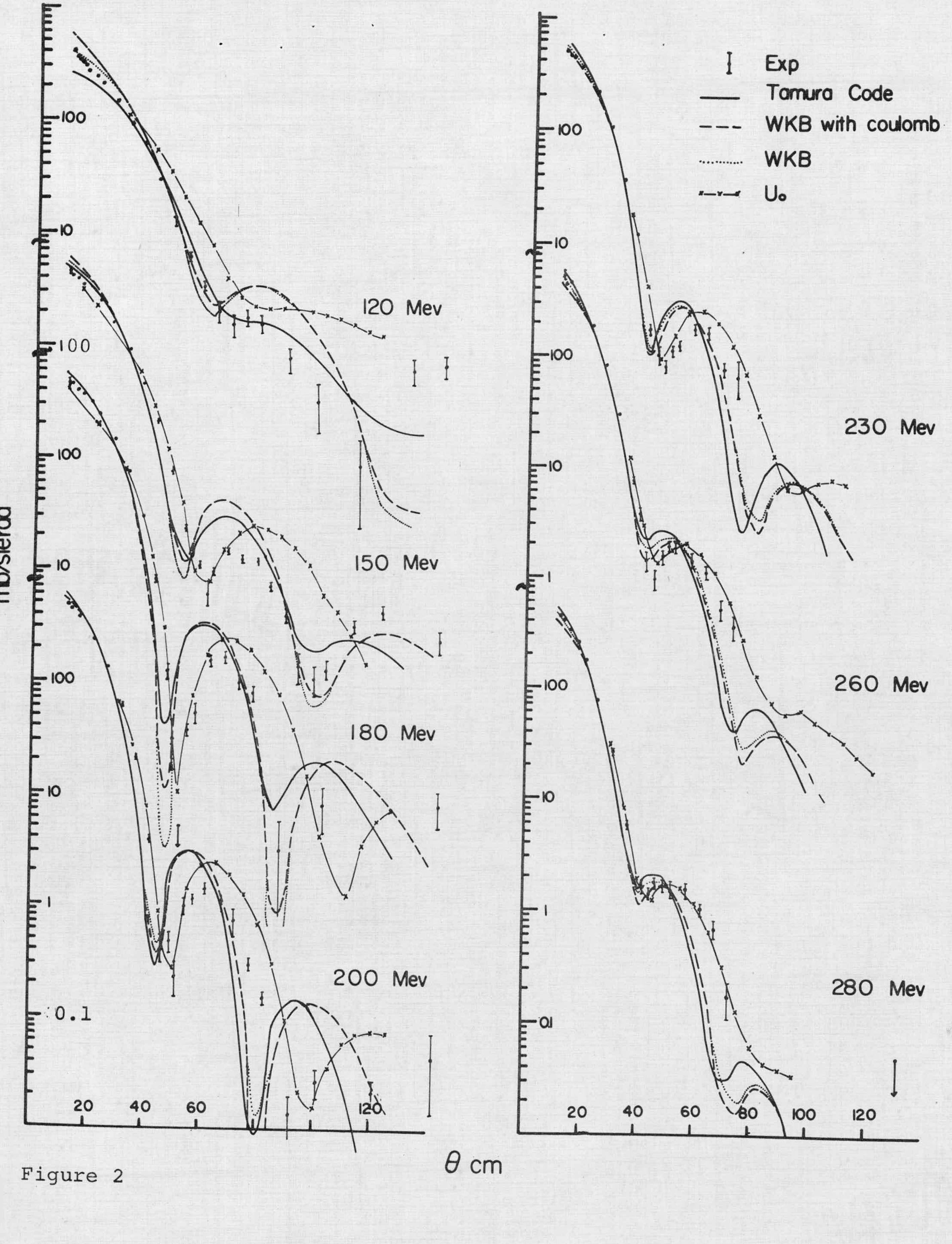

Exp
Tamura Code
WKB with coulomb
WKB
U₀
120 Mev
150 Mev
180 Mev
200 Mev
230 Mev
260 Mev
280 Mev
mb/sterad
θ cm

Figure 2

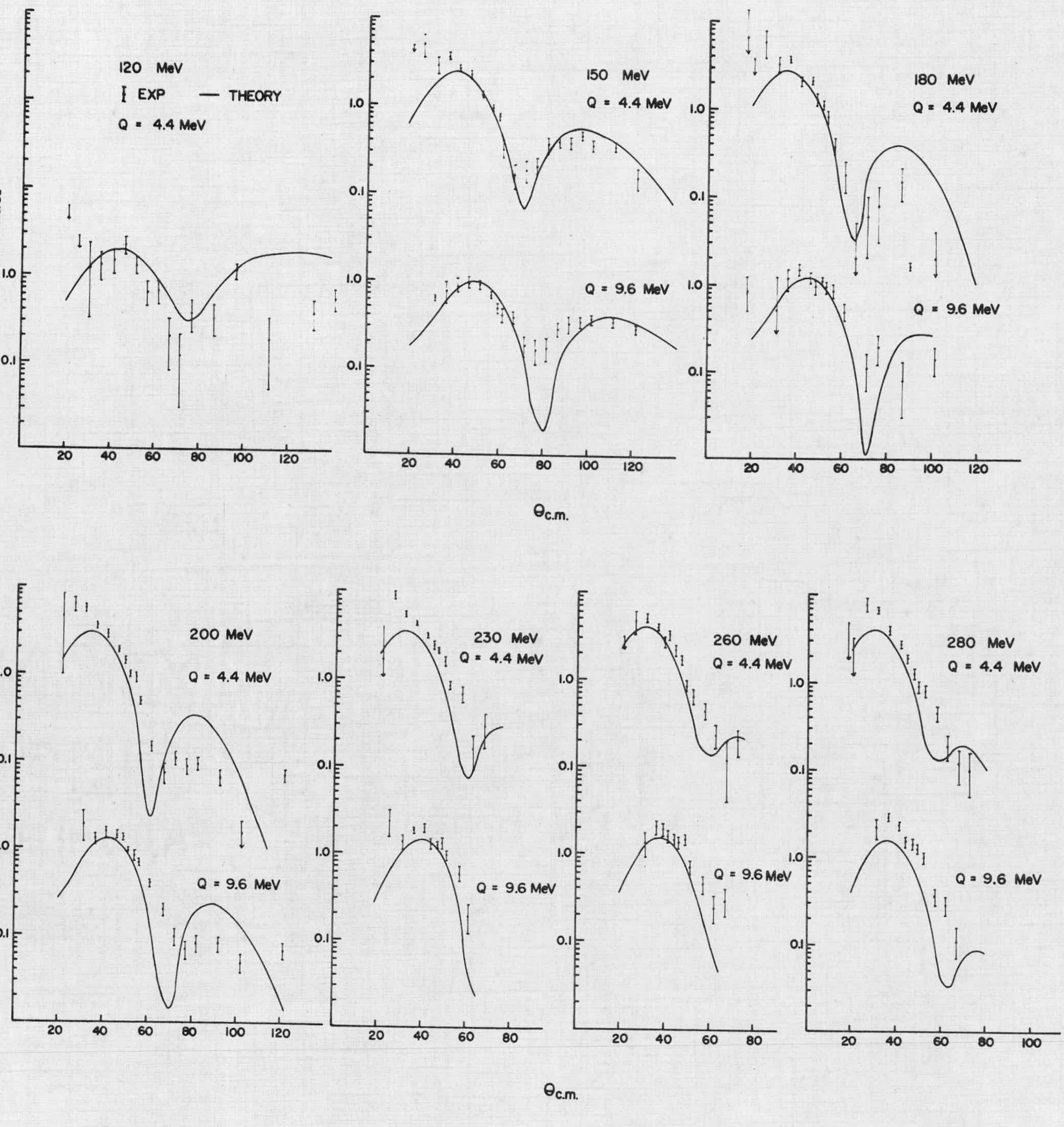
120 MeV
EXP — THEORY
Q = 4.4 MeV
150 MeV
Q = 4.4 MeV
Q = 9.6 MeV
180 MeV
Q = 4.4 MeV
Q = 9.6 MeV
200 MeV
Q = 4.4 MeV
Q = 9.6 MeV
230 MeV
Q = 4.4 MeV
Q = 9.6 MeV
260 MeV
Q = 4.4 MeV
Q = 9.6 MeV
280 MeV
Q = 4.4 MeV
Q = 9.6 MeV
mb/sterad
$\Theta_{c.m.}$

Figure 3